*IOSR Journal of Electrical and Electronics Engineering (IOSR-JEEE)*
*e-ISSN: 2278-1676,p-ISSN: 2320-3331, Volume 11, Issue 6 Ver. II (Nov. – Dec. 2016), PP 25-36*
*www.iosrjournals.org*

# Sizing, Modeling and Control of Photovoltaic Traffic Light System

Abd El-Fattah A. Omran[1], Faten H. Fahmy[1], Abd El-Shafy A. Nafeh[1], Hosam K. M. Yousef[2]
[1]*Photovoltaic cells Department, Electronic Research Institute, Cairo, Egypt*
[2]*faculty of Engineering, Cairo University*

***Abstract:*** *The applications of renewable energy systems have become very important in all domains nowadays. One of the most important applications is a Photovoltaic (PV) traffic light system. A traffic light system is considered to be one of the most critical applications that can solve the congestion problems of the streets. This paper presents a solution for the unpredictable repeated power failure for the traditional grid-connected traffic light systems by using stand-alone PV system. The proposed PV system consists of a PV array, a DC-DC converter, and a battery for backing up. Also, this paper gives a complete modeling, simulation and control of the PV Power system by using MATLAB-Simulink. The proposed control of the PV power system performs two functions that are maximum power point tracking (MPPT) for the PV system and battery charging. Moreover, this paper proposes a traffic light control technique that is based on comparing the densities of roads intersections by using LABVIEW software to control the traffic light signals. The obtained results show the effectiveness of the proposed control techniques.*
***Keywords:*** *Renewable energy, photovoltaic, traffic system control, maximum power point tracking.*

## I. Introduction

Getting clean, efficient, and harmless energy is one of the main challenges facing the world nowadays. Traffic problem is one of the critical problems that faces most of the countries in the world especially in the developing countries such as Egypt. The problem of the traditional grid-connected traffic light systems is the unpredictable repeated power failure, which arises due to lack of fossil fuel at generation stations. The photovoltaic (PV) is one of the optimum solutions for these systems, due to it is clean and sustainable energy source, has little maintenance, high reliability, no noise, no moving parts, and has also economic benefits. But, there are still two principal barriers to the use of PV systems: the high installation cost and the low energy conversion efficiency [1]. The output power of PV greatly depends on solar irradiance and temperature. Since, the current-voltage (I-V) characteristic curve of PV array varies with solar irradiance and temperature dynamically, it is crucial to operate PV array to a specific point to harvest maximum solar energy. Therefore, a maximum power point tracking (MPPT) algorithm, which can compute the most efficient operating point of the PV array is very important [2]. Directly connected PV systems operate at the intersection point of the (I-V) curves of the PV array and the load. This operating point may be far from the maximum power point (MPP) of the PV generator and thus wasting a significant amount of the available solar power. So, it is necessary to maximize the energy utilization of these systems via maximum power point tracking. A simple DC–DC converter controlled by an MPPT algorithm can be used as a controller to match the PV generator to the load [3]. The battery can be integrated into the PV system for storing the excess energy during the day light times and using it during periods of energy deficit. The charger controller is important part from the PV power system that charge batteries; its purpose is to keep the batteries properly fed and safe. The basic functions of the charge controller are blocking reverse current, prevent the batteries from overcharging and over discharging and thus increases the life time of the batteries [4], [5].

The congestion of the urban traffic is becoming one of the critical issues with the increasing population and number of vehicles in cities day by day. Traffic jams not only cause extra delay and stress for the drivers, but also increase fuel consumption, transportation cost, and air pollution. The traffic light system controller is one of the critical and important factors affecting the traffic flow in the streets and roads intersections. The traditional way for controlling traffic light systems is based usually on using timers with fixed times, which waste more time. Another method is to use the infrared sensors, which is considered to be one of the flexible vehicle detection methods. Nowadays, the developed intelligent traffic control systems which are based on the measurement of traffic densities on the road are considered to be the most common techniques [6], [7]. So it is necessary to utilize a new controller, instead of the traditional one, that can control the traffic light efficiently and rapidly. This control is based on comparing the congestion in the roads intersections and controls the traffic light signals according to the densities of the intersections. The traffic lights control system is built up by using LABVIEW graphical programing environment.

## II. Configuration of the PV Traffic Light System

The suggested stand-alone PV traffic light system comprises of two main systems that are the PV system and the traffic light system. The block diagram of the suggested stand-alone PV traffic light system is shown in Fig. 1. The main components of the suggested system are the PV array, the batteries, the MPPT, and battery charging controllers, traffic light control unit and DC load (300 W). Where, the function of the PV array is to convert the sunlight directly into DC electrical power, and that of the battery is to store the excess power from the PV array [8]. The MPPT controller is very important to operate PV to harvest the maximum solar energy. The traffic control system is used to control the traffic flow and manage the traffic light signals efficiently.

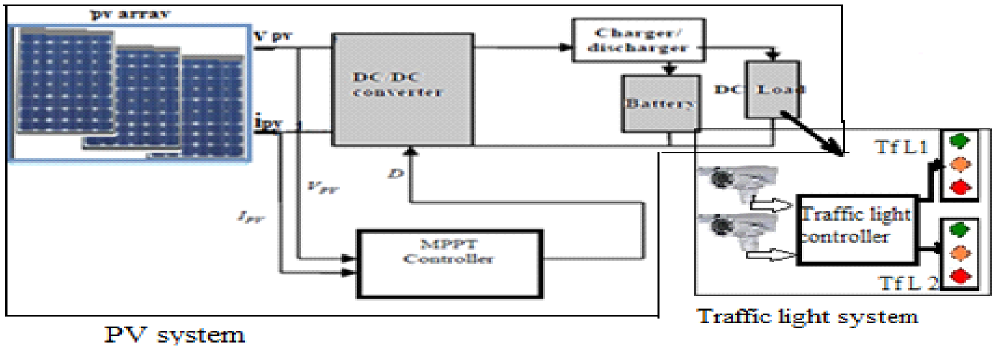


**Fig.1.**Block diagram of the PV traffic light system.

## III. The Stand-Alone PV System

The stand-alone PV system consists of the PV array, which is considered to be the only power source for supplying the load with the required electrical energy and the battery, which is considered to be the storage unit. Therefore, the stand-alone PV system must be carefully sized for keeping the system in continues operation.

### 3.1. PV System Sizing

There are two methods for sizing the PV system that are the simple numerical calculation method and the HOMER methods.

#### 3.1.1. PV sizing using numerical calculation method

#### 3.1.1.1. Array sizing

The size of the PV array can be estimated as follows: the PV panel area is, first, evaluated for one daily load energy requirements by Eq. (1) [8].

$$\text{PV (Area)}= \frac{E_L}{G_{avg} \times TCF \times \eta_{PV} \times \eta_{out}} \tag{1}$$

Where, $E_L$ is the demand energy, $G_{avg}$ is The average solar radiation input per day (kWh/m$^2$/day) for the studied location of the system which is Electronic Research Institute - Cairo - Egypt, *TCF* is the Temperature correction factor (0.8 for temperatures over the 60$^o$C), $\eta_{PV}$ is the PV module efficiency and $\eta_{out}$ is the Battery efficiency (85%).

The PV peak power at peak solar insolation (PSI) of 1000 W/m$^2$ is given by Eq. (2).

$$\text{PV (peak power)} = PV_{area} \times PSI \times \eta_{PV} \tag{2}$$

#### 3.1.1.2. Battery sizing

The selection of battery depends on two factors that are depth of discharge (DOD) of battery and system voltage. In solar PV, the deep discharge batteries are used with DOD in the range of 70%. The battery storage capacity can be calculated according to the following relation.

$$\text{Battery storage capacity (Ah)} = \frac{N_C \times E_L}{DOD \times \eta_{out}} \tag{3}$$

Where, $N_C$ is the Number of continuous cloudy days (2day). The specifications of the resulted PV system components are summarized in Table 1.

**Table 1.** Component specifications.

| Component | Capacity | Number of units | Characteristics |
| --- | --- | --- | --- |
| PV array | 1.80 kW | 12 (of $150W_p$ module) | 103.5 , 17.4 A |
| Battery | 20.168 kWh | 18 (of 12V 100Ah battery) | 24 ,840 Ah |

### 3.1.2. Homer method

HOMER solves any optimization problem predetermined value of energy not served, through minimizing the present value of the global cost and provides the optimum PV, and battery size using data of the available location and the load demand. Fig. 2 shows the implementation of the PV system in Homer, which composed of a PV generator, battery, and traffic DC load. Table 2 summarizes the optimization results of the Homer program for the suggested PV system.

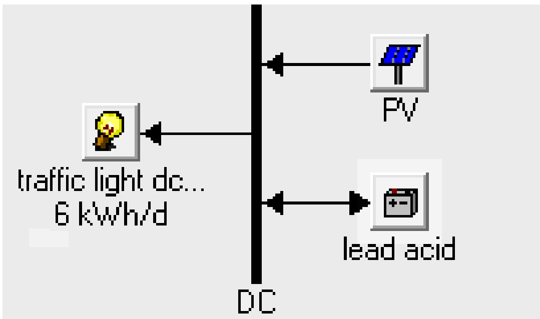


**Fig.2** Homer implementation of the PV system.

**Table 2.** Optimization results of homer program.

| PV (kW) | Battery (kWh) | Initial Capital | Operating Cost ($/yr) | Total NPC |
| --- | --- | --- | --- | --- |
| 1.700 | 21.600 | $5,880 | 2,291 | $28,844 |

## 3.2. Stand-Alone PV System Modeling

### 3.2.1. Modeling of the PV Array

A solar cell is a P-N junction fabricated in a thin wafer of semiconductor. The solar radiation can be directly converted to electricity through photovoltaic effect. Bp solar bpsx 150s PV module shown in Table 3 is chosen for MATLAB simulation. The module is composed of 72 multi-crystalline silicon solar cells connected in series and provides 150W of nominal maximum power [9].

**Table 3.** Electrical characteristics data of the used PV module.

| Electrical characteristics | Value |
| --- | --- |
| Maximum power ($P_{max}$) | 150W |
| Voltage at $P_{max}$ ($V_{max}$) | 34.5V |
| Current at $P_{max}$ ($I_{max}$) | 4.35A |
| Open circuit voltage ($V_{oc}$) | 43.5V |
| Short circuit current ($I_{sc}$) | 4.75A |
| Temperature coefficient of $I_{sc}$ | $0.065 \pm 0.015$ %/ $^{O}$C |
| Temperature coefficient of $V_{oc}$ | $-160 \pm 20$mV %/ $^{O}$C |
| Temperature coefficient of power | $-0.5 \pm 0.05$ %/ $^{O}$C |
| NOCT | $47 \pm 2^{O}$C |

The equivalent circuit model of a solar cell consists of a current generator and a diode plus series and parallel resistance as shown in Fig. 3. The mathematical expression of the output current of a single PV module is given by Eq. (4) [10].

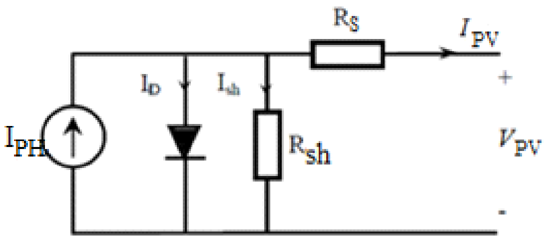


**Fig. 3The** equivalent circuit of solar cell.

$$I_{PV} = N_P I_{PH} - N_P I_o[\exp(q(\frac{V_{PV} + I_{PV} R_S}{N_S BKT}) - 1)] \quad (4)$$

Where, $V_{PV}$ is the output voltage of the PV module (V), $I_{PV}$ is the output current of the PV module (A), $I_{PH}$ is the light generated current (A), $I_o$ is the diode reverse saturation current, B is the ideality factor, K is the Boltzmann constant in J/K, q is the electron charge. $R_{sh}$ and $R_s$ are the shunt and series resistances of the cell, respectively. $N_S$ is the number of cells connected in series and $N_P$ is the number of cells connected in parallel.

### 3.2.2. DC-DC buck converter

The step down DC-DC converter, commonly known as a buck converter is shown in Fig. 4 [11]. A DC-DC converter is an electronic circuit which converts a source of direct current from one voltage level to another where the conversion ratio $V_{load} / V_{in}$ varies with the duty ratio D of the switch [12]. The buck converter is designed to operate in the continuous mode. Moreover, the DC-DC converter is used for maximum power point tracking.

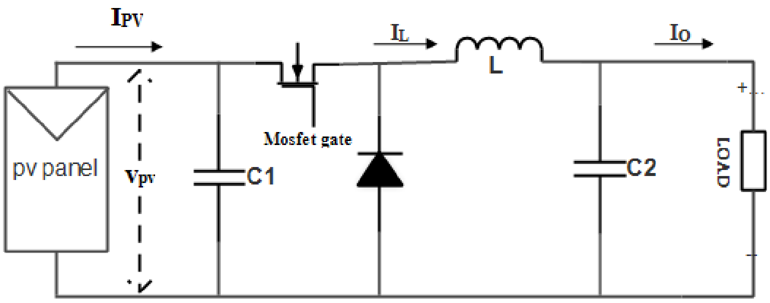


**Fig. 4** Schematic of the buck DC-DC converter.

### 3.2.3. Battery backup system

Due to the output of the solar supply is intermittent and changes unpredictably with solar insolation and ambient temperature. Thus, the battery energy storage is necessary to help to get a stable and reliable output from the PV for loads in the traffic systems. The terminal voltage ($V_1$,) of the battery is given by the Eq. (5) [5].

$$V_b = V_{oc} \pm I_b R \quad (5)$$

Where, $V_1$, $I_b$and$R_1$ are the battery open circuit voltage (V), battery current (A) and the internal resistance of the battery respectively. $V_{oc}$ and $R$ are governed by a set of equations depending on which mode of operation the battery is in. The battery is in charge mode when the battery input current is positive while the discharge mode is in case of the current is negative. For the lead acid battery storage subsystem implementation in Simulink, there is only one input to this subsystem ($I_b$) and the outputs of the system are battery voltage ($V_b$), battery power ($Pb$) and battery state of charge (SOC).

## 3.3. PV System Control

### 3.3.1. Maximum power point tracking algorithm

The output power of Photovoltaic varies with solar irradiance and temperature nonlinearly. Therefore, the MPPT is very important to operate PV to harvest the maximum solar energy in real time [2]. When a PV module is directly coupled to a load, the PV module's operating point will be at the intersection of its I–V curve and the load. As the PV module exhibits a nonlinear I-V characteristic and has a unique operating point that can extract maximum power from the module. Thus, to extract the maximum power from the PV and deliver it to the load, the PV internal impedance and load impedance should be match. To achieve this, it is necessary to add an adaptation device or a MPPT controller with a DC–DC converter between the PV source and the load. The MPPT acts to force the operating point of the PV module to track its peak power [1]. Many MPPT control techniques have been conceived for this purpose during the last decades. The different maximum power point tracking algorithms can be classified into [3]:

- Fractional Open Circuit Voltage.
- Fractional Short Circuit Current.
- Perturb and Observe (P&O).
- Incremental Conductance (INC).
- Artificial Intelligent method (Fuzzy logic control, neural network, etc…).

The Perturb and Observe (P&O) method is one of the most commonly used MPPT methods as it is simple and low cost. But the main problem is the output power fluctuation. The perturbation causes the power of the solar module changes. If the power increases due to the perturbation then the perturbation is continued in that direction. After the peak power is reached the power at the next instant decreases and hence after that the perturbation reverses. When the steady state is reached, the algorithm oscillates around the peak power point. In order to keep the power variation small the perturbation size is kept very small. It is clear that there are some power loss due to this perturbation also this algorithm fails to track the power under fast varying atmospheric conditions. The algorithm is developed in such a manner that it sets a reference voltage of the module corresponding to the peak voltage of the module. A PI controller then acts moving the operating point of the module to that particular voltage level [13]. In this work, the P&O based PI algorithm used to achieve the maximum power point tracking. Figure.5 illustrates the flowchart of the conventional P&O algorithm.

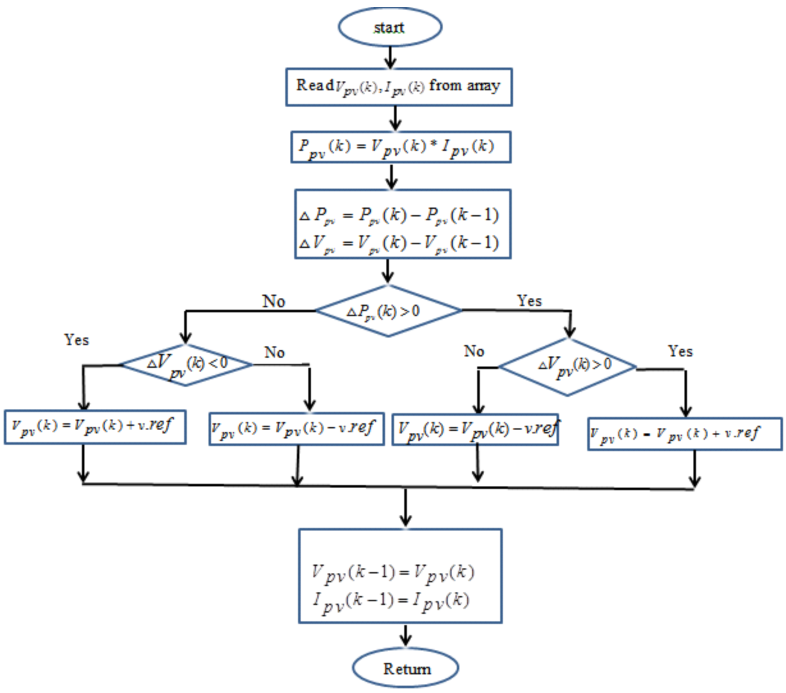


**Fig. 5** Flowchart of P&O MPPT algorithm.

**Charge Controller**

The charger controller in the stand-alone PV system is to maintain the battery at its highest possible state of charge and protect it from overcharging by the PV array and from over-discharging by the loads [14]. There are two modes of operation for the battery:

**Charge Mode**

The battery voltage and state of charge (SOC) during charging mode can be described using the following equations (6, 7):

$$V_{ch} = [2 + 0.148 \times SOC(t)] \times n_s \tag{6}$$

$$R_{ch} = \frac{0.758 + \dfrac{0.1309}{[1.06 \times SOC(t)] \times n_s}}{SOCm} \tag{7}$$

**Discharge Mode**

During discharging, the battery voltage and state of charge (SOC) relationships are given by:

$$V_{dch} = [1.926 + 0.124 \times SOC(t)] \times n_s \tag{8}$$

$$R_{dch} = \frac{0.19 + \dfrac{0.1307}{[SOC(t) - 0.14] \times n_s}}{SOC(m)} \tag{9}$$

Where, *SOC (t)* is the current state of charge, ns is the number of 2V battery cells in series and SOC(m) is the maximum battery capacity (Wh).

## IV. Traffic Light System

The traffic light, also known as traffic signal, traffic lamp, or semaphores, is a signaling device positioned at road intersections, crossing or other locations. Its purpose is to indicate, using a series of color (red, yellow, green) specific movement to drive, ride, or walk. The traffic light control system requires vehicle detection circuits, microprocessor embedded hardware, watchdog circuitry, and so on [15]. The traffic light is typically controlled by controller inside a cabinet mounted in a concrete pad. The control unit of the traffic light system is the most important unit to control the traffic flow and manage the traffic light signals efficiently.

### 4.1. Traffic Light System Control

Usually, the traffic light is controlled by the timer, which set relying on traffic in that area. But, in some areas the timer based system is not really efficient, because the appearance of vehicles are not constant. To overcome this problem, a new technique for control the traffic light system based camera sensors is used. The traffic light control strategy depends on images capturing, images recognition, and control the two intersections according to the numbers of objects. First, the image path entered, then the vision acquisition and vision assistant, which responsible for capturing the images and provides a means of converting the captured images to the IMAQ format for processing, to the LABVIEW picture format for display on the front panel [15]. The objects on the images are counted via count and measure objects tool. The system uses intelligent video cameras to capture real time visual images. From these images, information about the densities of the traffic and the number of vehicles will be extracted. The controller compares the numbers of objects in the two intersections and activates the traffic light signals of the congested intersection according to the densities of the objects in the two intersections. The control output signal is obtained by using LABVIEW software tools. This work is just only for control traffic light and not implementation for the complete traffic light system. Figure.6 shows the block diagram window of the traffic signal controller for the proposed system using LABVIEW software.

### 4.2. Traffic Light control cases

- If the number of the objects on the first intersection is larger than the number of the objects in the second intersection. The control signal activates the corresponding traffic light of the first congested intersection. Also, this will repeated with the second intersection.
- If the numbers of objects in the two intersections are equal, the priority is given to the first intersection.
- If the traffic light signal of one intersection is activated for continuous three cycles, the other traffic signal will be activated for one cycle, and then the system will continue its operations, where the cycle is about (60sec).

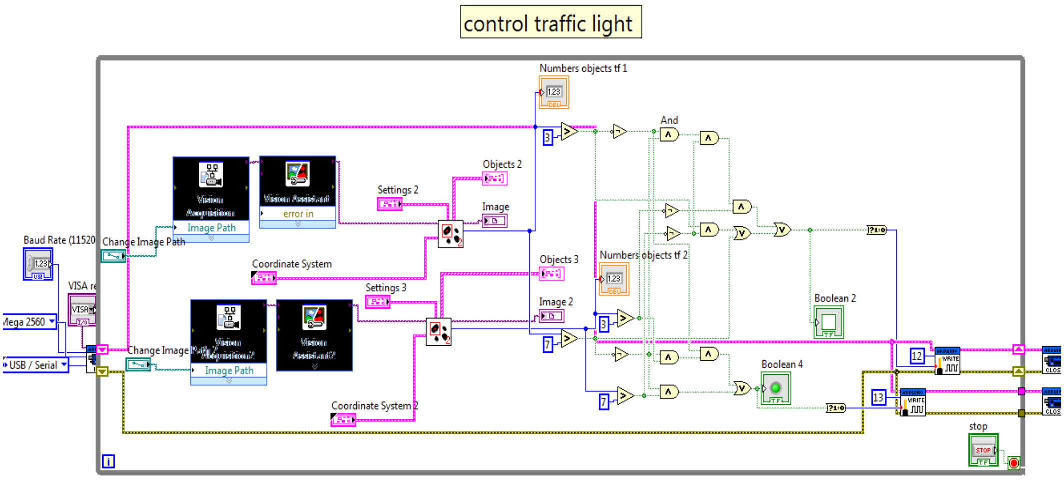


**Fig. 6** The block diagram window of the traffic signal controller using LABVIEW.

## V. Simulation and Results

The simulation results of the proposed system, which comprises of the PV system and traffic light system are shown in the following subsystem.

- **Results of the PV System**

The complete Simulink model of the PV system is shown in Fig.7. The modeled system consists mainly of the models of the PV array, the buck converter, the battery, the battery charger, the MPPT controller, and the load. The main modeled blocks are coupled to implement the complete model of the proposed PV system. Figures. 8 show the output characteristics for one PV module at different insolation levels and temperatures. Such Figs. (a) & (b) show the I-V characteristics and P-V characteristics of the PV module at different insolation levels and at constant temperature 25°C. Also, Figs. (c) & (d) show the I-V characteristics and P-V characteristics of the PV module at different temperatures and at constant insolation of 1000 W/m$^2$. It is clear from these figures that, the short circuit current increases dramatically with increasing the solar radiation. Also, the open circuit voltage decrease significantly with increasing the temperature.

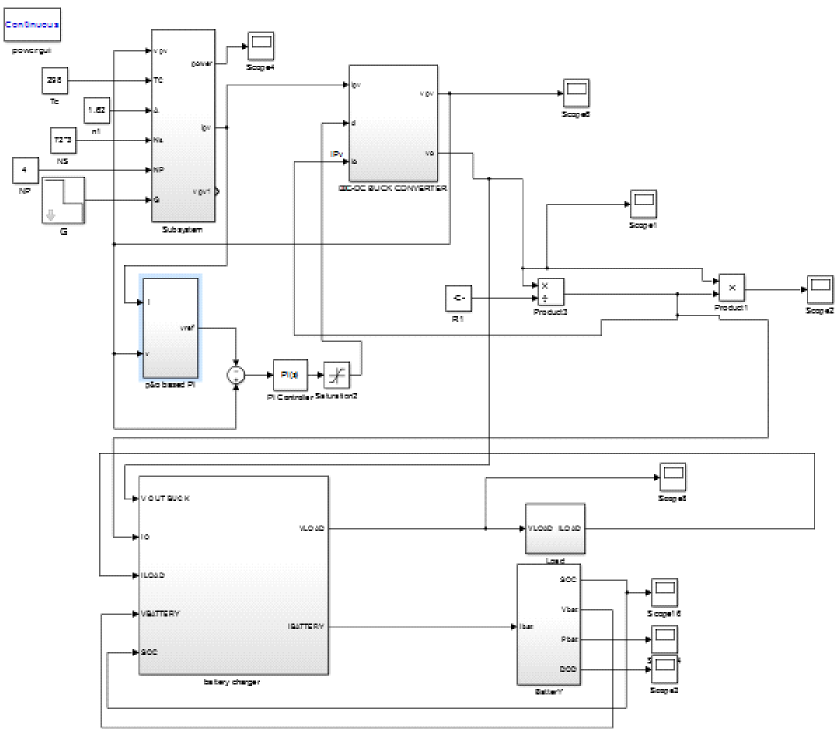

**Fig. 7** Complete Simulink model of the PV model.

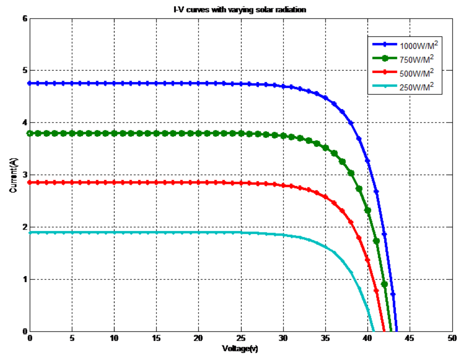

**(a) I-V** curves at different insolation levels.

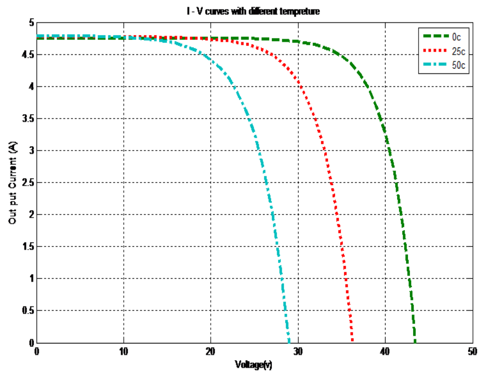

**(c) I-V** curves at different temperatures.

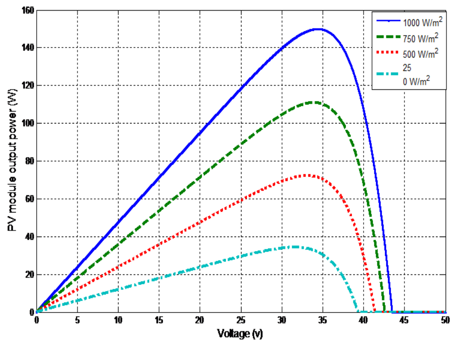

**(b) P-V** curves at different insolation levels.

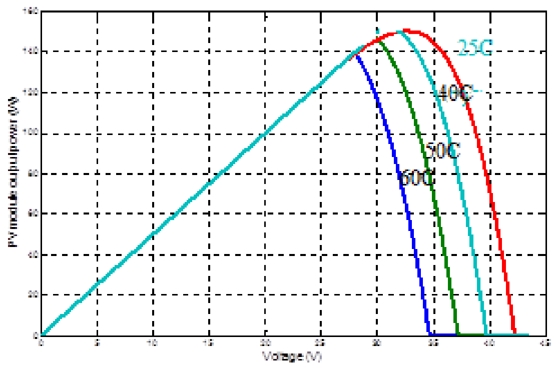


**(d) P-V** curves at different temperatures.

**Fig. 8** characteristics of the PV module.

Figure.9 shows the response of the PV module output power using P&O based PI MPPT at different values of the insolation and at constant temperature of 25$^{o}$C. It is clear, from this figure that, the used P&O based PI MPPT has high ability to track the different maximum power points of the PV module quickly.

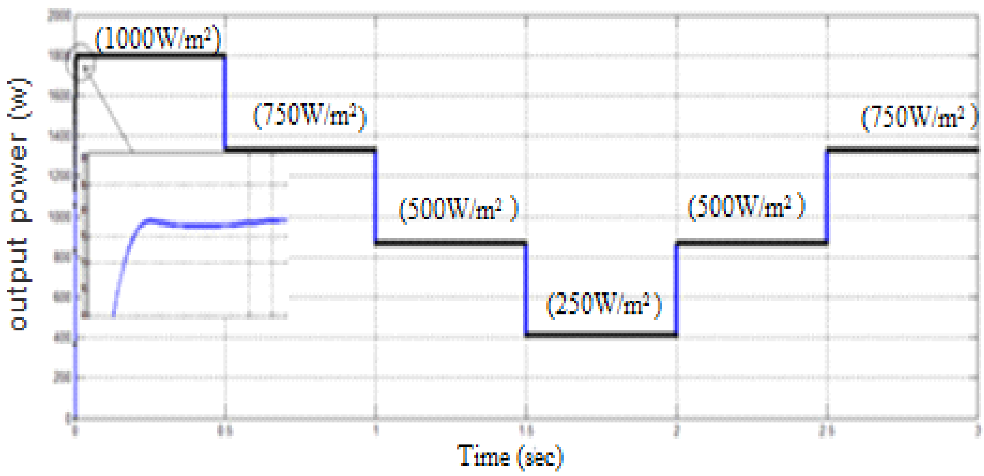


**Fig. 9** Array output power with P&O based PI MPPT.

Figure.10 shows a comparison between the dynamic response of the PV output power by using the conventional P&O and the utilized P&O based PI MPPT at 25 $^{o}$C and different insolation levels. It is shown from this figure that the proposed P&O based PI is more faster than the conventional P&O in the tracking the different maximum power points at sudden changes in insolation levels.

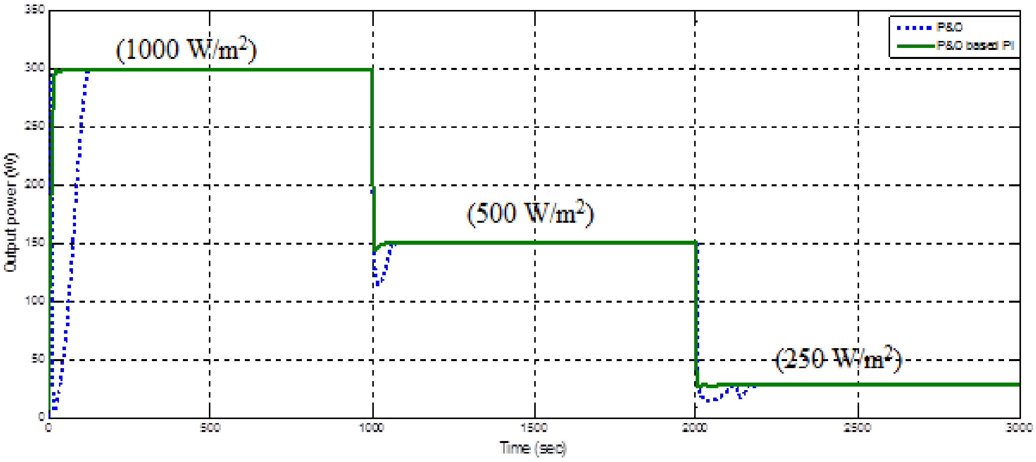


**Fig. 10** Comparison between PV output power with P&O and P&O based PI.

The overall stand-alone PV system model was simulated using radiation data of two cloudy and sunny days at constant temperature of 25$^{o}$C. Results are exhibited in two groups to show the performances of PV output power, DC load and the battery after using the P&O based PI MPPT controller. Fig. 11 (a) & (b) show the performance of the PV output power during cloudy day and sunny days respectively. The radiation increase gradually from 6:30 AM to noon then decrease gradually to the sun set 6:45 PM. It is clear that the output power of the PV array is proportional to the solar radiation level. Fig. 12& 13 show the performance of the DC load voltage and DC load power. Figs 14 &15 show the voltage and current performances of the battery in cloudy and sunny days respectively, while the DC load and battery voltages are independent on the solar radiation and exist all over the 24 hours. It can be shown that the battery discharge with negative sign of the current during the nighttime till the sun rises. When the sunrises and solar radiation begins to increase, the PV output power feeds the DC load with the excessive energy from the PV charge the battery during this period of radiation with positive sign current. Fig. 16 (a) & (b) indicate the state of charge of the system battery during the sunny and cloudy days, respectively. When the battery full charged the battery current will be zero and the SOC remain 100% for this time period till the generated power by the PV is less than the power needed by the load, then the battery can deliver the power to the load and the SOC will decrease.

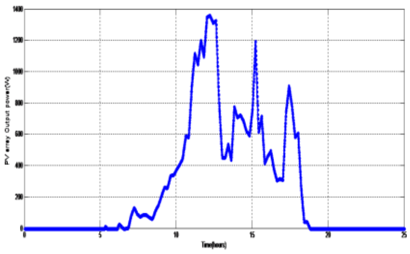

**(a)** Output power of PV During cloudy day

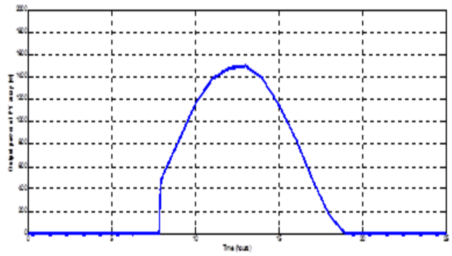

**(b)** Output power of PV During sunny day

**Fig. 11** Performance of the PV output power.

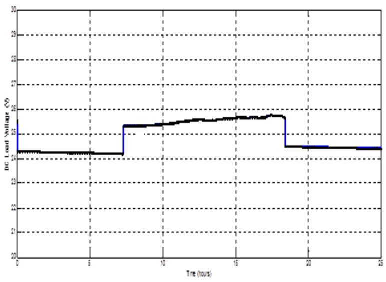

**(a)** DC Load voltage During cloudy day

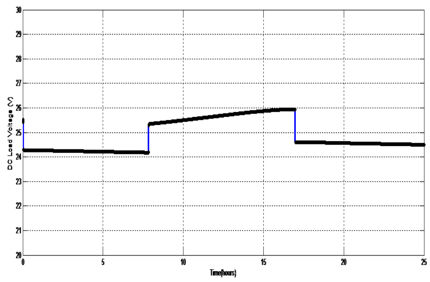

**(b)** DC Load voltage During sunny day

**Fig. 12** Performance of the DC Load voltage.

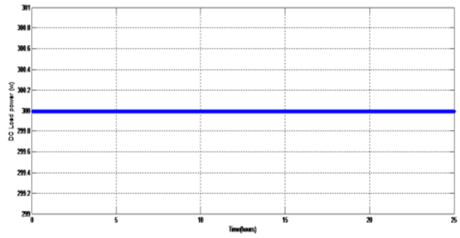

**(a)** DC Load power During cloudy day

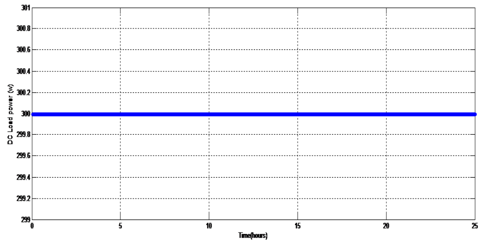

**(b)** DC Load power During sunny day

**Fig. 13** Performance of the DC Load power.

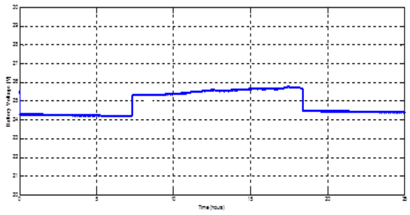

**(a)** Battery voltage During cloudy day

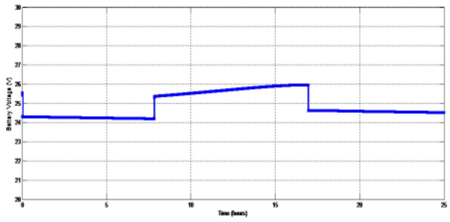

**(b)** Battery voltage During sunny day

**Fig. 14** Performance of the Battery voltage.

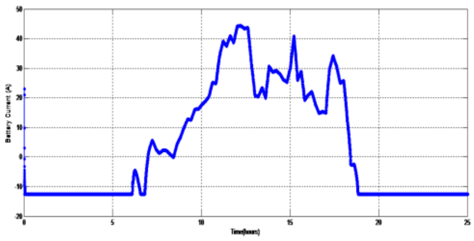

**(a)** Battery current During cloudy day

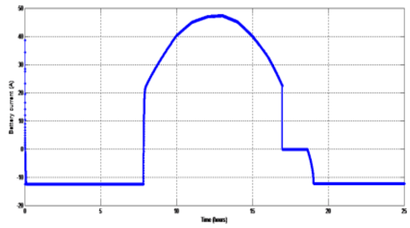

**(b)** Battery current During sunny day

**Fig. 15** Performance of the Battery current.

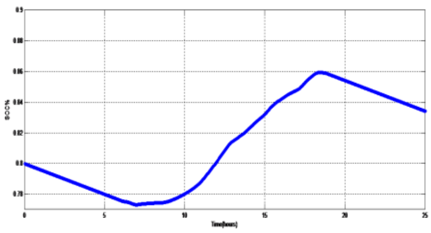

(a) SOC % During cloudy day

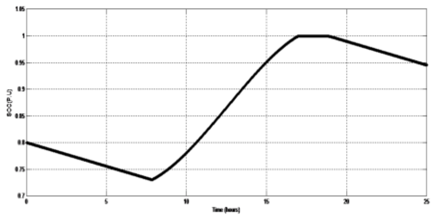

(b) SOC % During sunny day

**Fig. 16** Performance of the Battery current.

- **Results of the Traffic Light System Control**.

The performance of the traffic light system control at different densities using LABVIEW software will be shown in the following cases. Also, the numbers of vehicles and the control cases are shown in Tabel.4. Case (1), the numbers of vehicles in the first intersection are11, which they are larger than the numbers of vehicles in the second intersection, which they are 3. The traffic light of the first intersection is activated as shown in the front panel of the program in Fig. 17. In case (2), the traffic light of the second intersection is activated as the numbers of vehicles are larger than the numbers of vehicles in the first intersection which shown in Fig.18. Also, in case (3) the numbers of vehicles are equal in the both intersections (11) the priority given to the first intersection as shown in Fig.19. The simulation results show that the proposed technique is more accurate for counting objects, comparing the intersections densities and control the traffic light signals. Also, the average wait time of the proposed scheme is significantly less than that of the fixed time scheme. It can dynamically adjust the delay for green light and change the cycle of signal light according to the real time traffic flow.

**Table 4.** Traffic light signal Control cases

| Control cases | Number of vehicles in intersection 1 | Number of vehicles in intersection 2 | The activated Traffic light signal |
|---|---|---|---|
| Case1 | 11 | 3 | Traffic light of intersection 1 |
| Case2 | 6 | 11 | Traffic light of intersection 2 |
| Case3 | 11 | 11 | Traffic light of intersection 1 for priority |

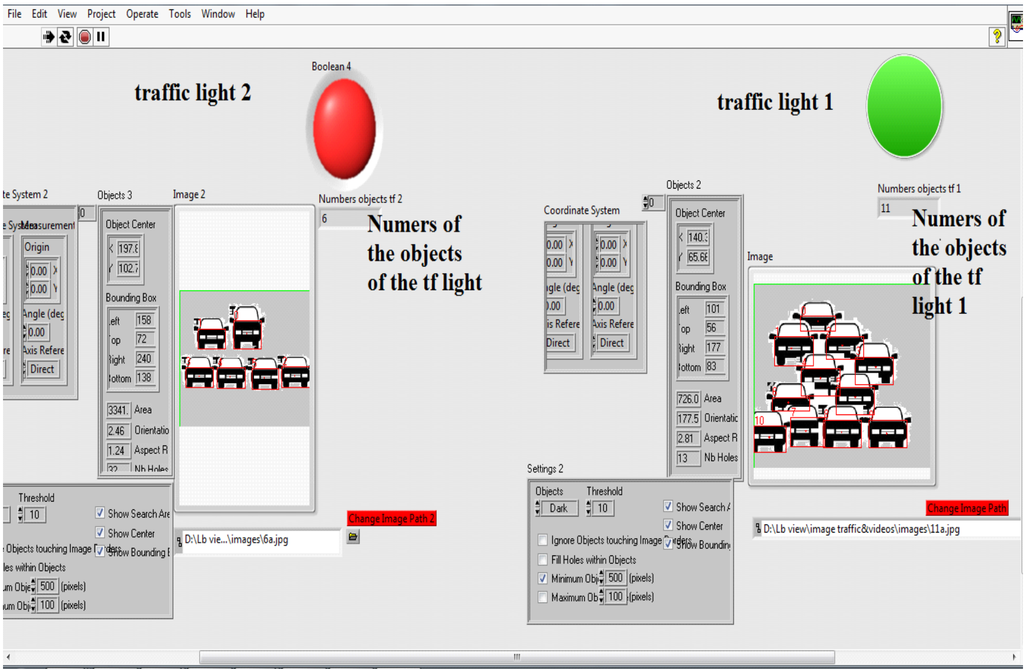


**Fig. 17** LABVIEW front panel for different control cases of the traffic system for the numbers of vehicles in the first intersection are larger.

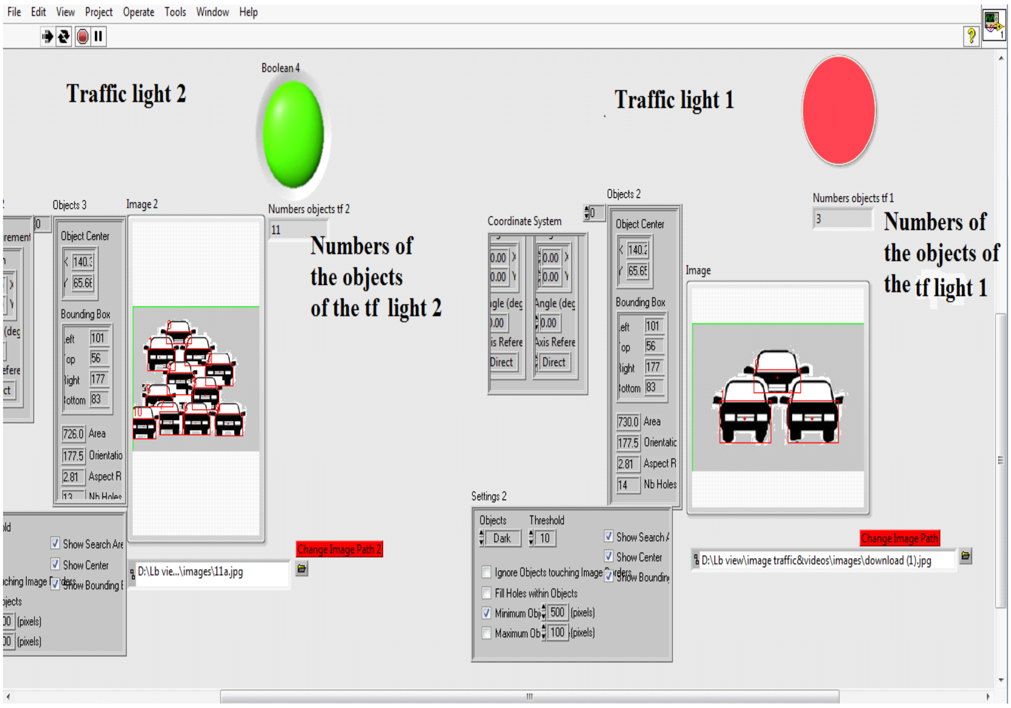


**Fig. 18** LABVIEW front panel for different control cases of the traffic system for the numbers of vehicles in the second intersection are larger.

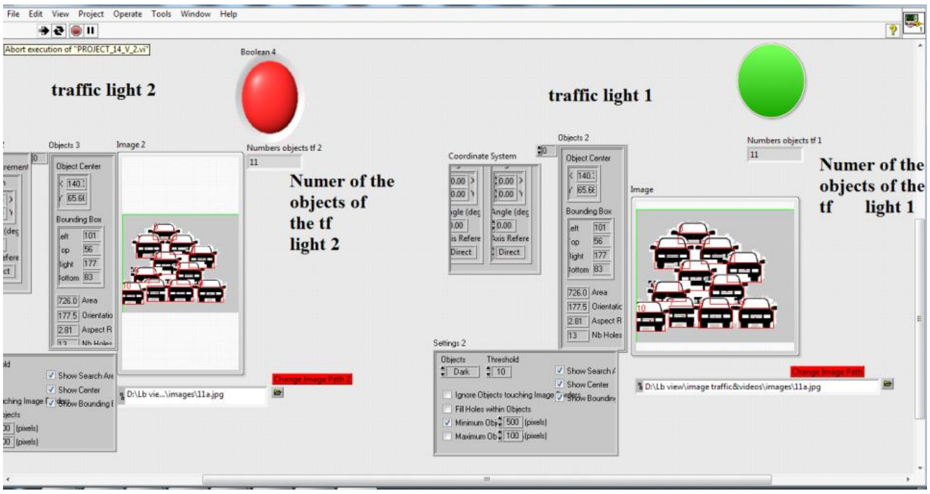


**Fig. 19** LABVIEW front panel for different control cases of the traffic system for the numbers of vehicles in the two intersections are equal.

## VI. Conclusions

This paper presented a configuration and design for a stand-alone PV traffic light system. Also, it presented two methods for sizing of the PV system that are HOMER method and simple calculation methods. A simulation model was designed for the stand-alone PV system by using MATLAB-Simulink. Moreover, this paper presented a comparison between two MPPT techniques that are conventional P&O and P&O based PI MPPT technique. At the same time, a proposed model of the traffic light system is designed for calculating and comparison of the densities of the vehicles in the two intersections by using LABVIEW tools. The simulation results of the comparison of these two MPPT techniques showed that the P&O based PI MPPT gave good and fast response compared to the conventional P&O MPPT with no oscillation at steady state. At the same time, the results show that the PV system with MPPT can feed the loads and battery with better performance at all levels of insolation. The use of MPPT technique with the battery charger controller in battery charging and the discharge present benefits to the life duration of the lead acid batteries. Moreever, simulation results of the traffic light system show that the traffic lights can be adjusted according to the real time traffic flow and the problem of the fixed time traffic light can be overcome. Finally, the proposed controller for the traffic system is simple, realized, and can solve the traffic problem.

## References

[1]. José A. Vieira, Alexandre M. Mota, "Implementation of a Stand-Alone Photovoltaic Lighting System with MPPT Battery Charging and LED Current Control," IEEE International Conference on Control Applications, September, 2010.
[2]. Jen-HaoTeng, Wei-Hao Huang, Tao-An Hsu and Chih-Yen Wang, "Novel and Fast Maximum Power Point Tracking for Photovoltaic Generation," IEEE Transactions On Industrial Electronics, March, 2016.
[3]. Mohamed M. Algazar, Hamdy AL-monier, and Hamdy Abd EL-halim, "Maximum power point tracking using fuzzy logic control," International Journal of Electrical Power & Energy Systems · July 2012.
[4]. Jaya. N, Madhuri. A "PIC Based Solar Charging Controller For Battery," International Journal of Engineering Science and Technology Vol. 4, No.02 February 2012
[5]. M. Makhlouf, F. Messai1, H. Benalla "Modeling and Simulation of Grid-connected Hybrid Photovoltaic/Battery Distributed Generation System," Canadian Journal on Electrical and Electronics Engineering Vol. 3, No. 1, January 2012.
[6]. N. Abbas, M. Tayyab, and M. Qadri "Real Time Traffic Density Count using Image Processing," International Journal of Computer Applications Vol.83 , No 9, December. 2013.
[7]. Jing pang, "Review of Microcontroller Based Intelligent Traffic Light Control," Emerging Technologies for a Smarter World (CEWIT), 2015 12th International Conference, IEEE, Oct. 2015.
[8]. Aicha Soufi, Ali Chermitti, N. B. Triki, "Sizing and Optimization of a Livestock Shelters Solar Stand-Alone Power System," International Journal of Computer Applications, Vol. 71– No.4, May 2013.
[9]. BP Solar BPSX150 – 150W.Multi-crystalline photovoltaic module datasheet,2001.
[10]. R. Ramaprabha, B. L. Mathur, and M. Sharanya "Solar Array Modeling and Simulation of MPPT using Neural Network," IEEE Trans. Energy Convers, vol. 22, No. 2, pp. 439–449, Jun. 2007.
[11]. Dariusz czarkowski elements of power electronics 1998 new york oxford university.
[12]. T. Esram and P. L. Chapman, "Comparison of photovoltaic array maximum power point tracking techniques," IEEE Transactions on Energy Conversion, VOL. 22, NO. 2, JUNE 2007.
[13]. Vikrant. A. Chaudhari, "Automatic Peak Power Tracker for Solar PV Modules Using dSPACE$^{R}$ Software," in Maulana Azad National Institute Of Technology Vol. Degree of Master of Technology In Energy. Bhopal: Deemed University, 2005, pp. 98.
[14]. Anca D. Hansen, Poul Sorenson, Lars H. Hansen, and Henrik Bindner, 2000,"Models of stand-alone PV System," Riso Ntional Laboratory, Roskilde.
[15]. Christopher G. Relf, "Image acquisition and processing with LABVIEWTM,". CRC press, 2003.